

# ERK-modulated intrinsic signaling and G<sub>2</sub>/M phase arrest contribute to the induction of apoptotic death by allyl isothiocyanate in MDA-MB-468 human breast adenocarcinoma cells

SHIH-CHANG TSAI<sup>1</sup>, WEN-WEN HUANG<sup>1</sup>, WEI-CHIEN HUANG<sup>3</sup>, CHI-CHENG LU<sup>5</sup>, JO-HUA CHIANG<sup>5</sup>, SHU-FEN PENG<sup>1</sup>, JING-GUNG CHUNG<sup>1</sup>, YU-HSIN LIN<sup>1</sup>, YUAN-MAN HSU<sup>1</sup>, SAKAE AMAGAYA<sup>4,6</sup> and JAI-SING YANG<sup>2</sup>

Departments of <sup>1</sup>Biological Science and Technology, and <sup>2</sup>Pharmacology, <sup>3</sup>Graduate Institute of Cancer Biology, <sup>4</sup>Tsuzuki Institute for Traditional Medicine, China Medical University, Taichung 404; <sup>5</sup>Department of Life Sciences, National Chung Hsing University, Taichung 402, Taiwan, R.O.C.; <sup>6</sup>Department of Kampo Pharmaceutical Sciences, Nihon Pharmaceutical University, Saitama 362-0806, Japan

Received May 24, 2012; Accepted August 28, 2012

DOI: 10.3892/ijo.2012.1640

**Abstract.** Allyl isothiocyanate (AITC), a member of the isothiocyanate (ITC) family found in a constituent of cruciferous vegetables, possesses anticancer activity and induces apoptosis in various types of human cancer cell lines. However, no available information showed antitumor effects in human breast adenocarcinoma cells. The current study was focused on exploring the mechanisms underlying AITC-induced apoptosis in MDA-MB-468 human breast cancer cells *in vitro*. We found that AITC reduced the cell number and viability using trypan blue staining with the Countess Automated Cell Counter and the MTT assay, respectively. AITC also was found to induce apoptotic cell morphological changes by a contrast-phase microscope and cell cycle arrest at G<sub>2</sub>/M phase by flow cytometric assay in MDA-MB-468 cells. Intrinsic apoptosis-associated factors such as caspase-9 and caspase-3 activities were performed, and reactive oxygen species (ROS) production, loss of mitochondrial membrane potential ( $\Delta\Psi_m$ ) occurred in AITC-treated MDA-MB-468 cells. AITC also stimulated mitochondria-related signaling, including p-Bcl-2 (Ser-70), cytochrome *c* and Apaf-1 in MDA-MB-468 cells. We found that the p-ERK signal was upregulated in AITC-treated cells. Importantly, NAC (a ROS scavenger) and U0126 (an ERK inhibitor) abolished AITC-reduced viability in MDA-MB-468 cells. AITC downregulated CDK1 activity and

altered the expression of G<sub>2</sub>/M phase-modulated associated protein levels by western blotting in MDA-MB-468 cells. In summary, our findings demonstrated that AITC-promoted G<sub>2</sub>/M phase and AITC-triggered apoptosis correlate with the activation of phosphorylation of ERK in MDA-MB-468 cells. AITC is a potential agent for application in the treatment of human breast cancer.

## Introduction

Allyl isothiocyanate (AITC) is a compound of the natural isothiocyanates found in cruciferous vegetables such as brussels sprouts, cauliflower, cabbage, kale, horseradish and wasabi (1-4). AITC is known to have multiple effects such as antipathogenic bacteria (5), anti-inflammatory (6), anti-fungicidal (7) and anticancer activities (4). Previous studies have demonstrated that AITC exhibits significant antitumor activities against human prostate (8), colorectal (9,10), bladder (11,12), cervical cancer cells (13) and leukemia cells (14). The anticancer activities by AITC are involved in the induction of cell cycle arrest and apoptosis as well as inhibition of cell metastasis (15-17). Our previous study demonstrated that AITC triggers G<sub>2</sub>/M phase arrest and apoptosis in human brain malignant glioma GBM 8401 cells (16). However, there is no report addressing whether or not AITC inhibits cell proliferation, promotes cell cycle arrest and induces apoptosis in human breast adenocarcinoma cells.

Breast cancer is one of the leading causes of death in women worldwide (18). According to statistical results from GLOBOCAN in 2008 year, about 1.38 million new patients were diagnosed in breast cancer, and 458,400 people died from breast cancer in the worldwide (19). In Taiwan, 14.8 per 100,000 women die from breast cancer each year according to the Department of Health in 2010. Breast cancer cells that lack of estrogen receptor (ER), progesterone receptor (PR), and human EGF receptor 2 (*HER-2/neu*) expressions are known as

---

*Correspondence to:* Dr Jai-Sing Yang, Department of Pharmacology, China Medical University, No 91, Hsueh-Shih Road, Taichung 40402, Taiwan, R.O.C.  
E-mail: jaising@mail.cmu.edu.tw

**Key words:** AITC, apoptosis, G<sub>2</sub>/M phase arrest, mitochondria, ERK, human breast cancer MDA-MB-468 cells

triple negative breast cancer (TNBC) (20,21). TNBC is the most clinically invasive breast cancer and the characteristics are more invasive, less responsive to chemotherapy agents and associated with poorer prognosis (22). The current therapy for TNBC includes surgery and systemic chemotherapy but the clinical treatment is still unsatisfactory (23). Discovering TNBC therapeutic agents from dietary natural products provides a useful application and chemo-preventive or chemotherapeutic effectiveness on TNBC (24,25). The goal of this study was to explore whether the anti-TNBC activity of AITC mediates through the direct cytotoxic effects and to understand the molecular mechanisms in human breast adenocarcinoma MDA-MB-468 cells. This study is focused on the cell cycle arrest and apoptotic cell death-induced by AITC in the MDA-MB-468 cells. Our data demonstrated that AITC inhibits cells viability, induces apoptotic death, and simultaneously causes cell cycle arrest in G<sub>2</sub>/M phase through the extracellular signal-regulated kinase (ERK) signaling pathway in MDA-MB-468 cells.

## Materials and methods

**Chemicals.** AITC, propidium iodide (PI), dimethyl sulfoxide (DMSO), RNase A, *N*-acetyl-L-cysteine (NAC), U0126 and Triton X-100 were purchased from Sigma-Aldrich Corp. (St. Louis, MO, USA). The fluorescent probes 2',7'-dichlorofluorescein diacetate (H<sub>2</sub>DCF-DA) and 3,3'-dihexyloxycarbocyanine iodide DiOC<sub>6</sub>(3), Dulbecco's modified Eagle's medium (DMEM), L-glutamine, fetal bovine serum (FBS), penicillin-streptomycin and trypsin-EDTA were obtained from Life Technologies (Carlsbad, CA, USA). Anti-p-ERK, anti-ERK, anti-Bcl-2, anti-p-Bcl-2 (Ser-70), anti-cytochrome *c*, anti-Apaf-1, anti-cyclin B and anti-CDK1 and second antibodies were purchased from Santa Cruz Biotechnology Inc. (Santa Cruz, CA, USA). Anti-p21/WAF-1 (Cat. 05-345) and Immobilon Western Chemiluminescent HRP substrate (Cat. WBKLS0500) were bought from Merck Millipore Corp. (Bedford, MA, USA).

**Cell culture.** Human breast adenocarcinoma MDA-MB-468 cell line was made by Dr Wei-Chien Huang (Graduate Institute of Cancer Biology, China Medical University, Taichung, Taiwan). Cells were placed into 75-cm<sup>2</sup> tissue culture flasks under a humidified 5% CO<sub>2</sub> and 95% air grown at 37°C and one atmosphere in DMEM supplemented with 10% FBS, 2 mM L-glutamine, 100 U/ml penicillin and 100 µg/ml streptomycin. Subconfluent cells (80%) were passaged with a solution containing 0.25% trypsin and 0.02% EDTA.

**Determinations of cell number and cell viability.** Cells at a density of 2x10<sup>5</sup> were seeded in 12-well plates and then exposed to 5, 10, and 20 µM AITC or 0.1% DMSO (as a vehicle control) for 24 and 48 h, then the cells were harvested and the cell number determined using trypan blue stain by Countess Automated Cell Counter (Invitrogen/Life Technologies) (26,27). Cells were incubated with or without 5, 10 and 20 µM of AITC for 24 and 48 h in presence and absence of NAC (a ROS scavenger) or U0126 (an ERK inhibitor). Cells were determined for viability utilizing thiazolyl blue tetrazolium bromide (MTT) assay as previously described (28,29). Each data point was represented from three independent experiments.

**Cell morphological analysis.** Approximately 2x10<sup>5</sup> cells/well of MDA-MB-468 cells in 12-well plates were incubated with or without 20 µM AITC and equal amount of DMSO as a control for 24 h at 37°C. At the end of treatment, cells were examined and photographed under a phase-contrast microscope at a x200 magnification for examining the cell morphological changes (30,31).

**Analysis for cell cycle distribution and sub-G<sub>1</sub> population.** Approximately 2x10<sup>5</sup> cells/well of MDA-MB-468 cells in 12-well plates were incubated in presence and absence of 5, 10 and 20 µM AITC then were placed in an incubator for 24 h, and then cells were harvested by centrifugation at 1,000 x g for 5 min, pellet were washed twice with cold PBS then fixed gently by 70% ethanol at 4°C overnight. Then cells were washed twice with cold PBS then resuspended in PBS containing 40 µg/ml PI and 0.1 mg/ml RNase A and 0.1% Triton X-100 in the dark for 30 min at 37°C then the cells were analyzed with a flow cytometer (FACSCalibur, BD Biosciences, San Jose, CA, USA) equipped with an argonion laser at 488 nm wavelength. Then the cell cycle and sub-G<sub>1</sub> (apoptosis) group were determined and analyzed (32,33).

**Caspase-9 and -3 activity assays.** About 5x10<sup>6</sup> cells of MDA-MB-468 cells in 75-T flasks were treated with or without 5, 10, 15 and 20 µM of AITC, then incubated for 12 h to detect the activity of caspase-9 and -3 which was assessed according to manufacturer's instruction of the Caspase colorimetric kit (R&D Systems Inc., Minneapolis, MN, USA). Cells were harvested and lysed in 50 µl lysis buffer containing 2 mM DTT, for 10 min. After centrifugation, the supernatant containing 200 µg protein were incubated with caspase-9 and -3 substrates in reaction buffer. Then all samples were incubated in a 96-well flat bottom microplate at 37°C for 1 h. Levels of released pNA were measured with ELISA reader (Anthos Labtec Instruments GmbH, Salzburg, Austria) at 405 nm wavelength (34,35).

**Detections of reactive oxygen species (ROS) and mitochondrial membrane potential (ΔΨ<sub>m</sub>).** MDA-MB-468 cells (2x10<sup>5</sup> cells/well) in 12-well plates with 0, 5, 10, 15 and 20 µM of AITC were incubated for 12 h to determine the changes of ROS production and ΔΨ<sub>m</sub> levels. The cells were harvested by centrifugation and were washed twice by PBS, then were resuspended in 500 µl of H<sub>2</sub>DCF-DA (10 µM) and 500 µl of DiOC<sub>6</sub>(3) (1 µmol/l) and incubated at 37°C in the dark for 30 min and were analyzed immediately by flow cytometry as described previously (32,33).

**Western blot analysis.** MDA-MB-468 cells at a density of 5x10<sup>6</sup> cells/ml seeded into T-75 flasks were treated with 5, 10 and 20 µM of AITC for 2 and 12 h. Cells were harvested from each treatment then were washed with cold PBS and then scraped and washed twice by centrifugation at 1,000 x g for 5 min at 4°C. All pellets were individually resuspended in the PRO-PREP protein extraction solution (iNtRON Biotechnology, Seongnam-si, Korea) for 3 h at -20°C as described previously (36,37). The lysate from each sample was collected by centrifugation at 12,000 x g for 30 min at 4°C, and the supernatant was stored at -20°C. Sodium dodecyl sulfate-polyacrylamide electrophoresis (SDS-PAGE) gels were used to separate proteins before

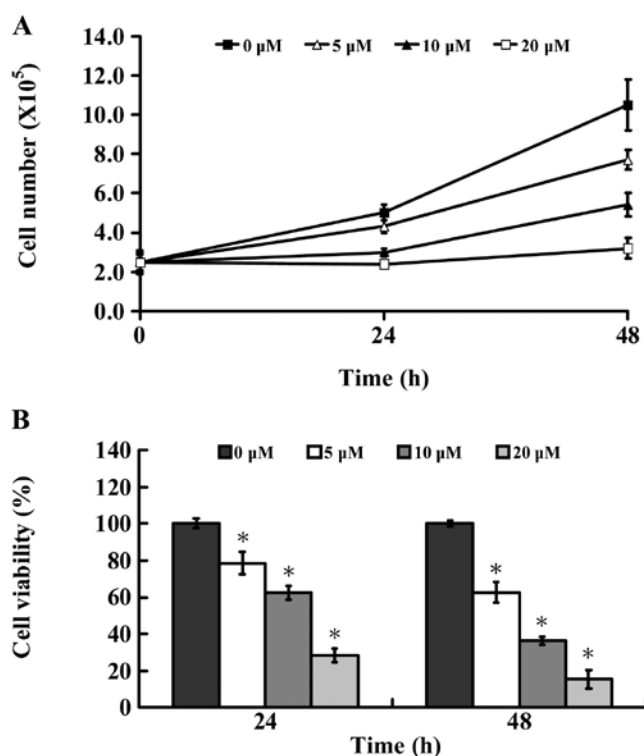


Figure 1. AITC reduces cell number and viability in MDA-MB-468 cells. Cells were incubated with 0, 5, 10 and 20  $\mu\text{M}$  of AITC for 24 and 48 h. (A) For cell number determination, cells were stained with trypan blue and determined by Countess Automated Cell Counter. (B) Cells were collected and were analyzed for viability by MTT assay as described in Materials and methods. Each point is mean  $\pm$  SD in triplicate. \* $p < 0.05$  was considered as statistically significant when compared with the untreated control (0  $\mu\text{M}$ ).

each sample was incubated with the primary antibodies (Santa Cruz Biotechnology Inc.) followed by secondary antibodies. These blots were then detected by Immobilon Western Chemiluminescent HRP substrate (Merck Millipore Corp.) and autoradiography using X-ray film (GE Healthcare, Piscataway, NJ, USA) (38,39). Each Immobilon-P transfer membrane (Cat. IPVH00010, Merck Millipore) was stripped and reprobbed with anti- $\beta$ -actin antibody as the loading control for ensuring that equal proteins were loaded (40,41).

**Determination of CDK1 kinase activity.** MDA-MB-468 cells were seeded onto 75-T flask and then treated with 0, 5, 10 and 20  $\mu\text{M}$  of AITC for 12 h. MDA-MB-468 cells were suspended in a final volume of 0.2 ml buffer containing 20 mM Tris-HCl (pH 8.5), 150 mM NaCl, 0.2% NP-40, 1 mM DTT, 1 mM EDTA, 1 mM EGTA, 0.2 mM PMSF, 1  $\mu\text{g}/\text{ml}$  pepstatin, 0.5  $\mu\text{g}/\text{ml}$  leupeptin, 5 mM  $\beta$ -glycerophosphate, 5 mM NaF, 1 mM  $\text{Na}_3\text{VO}_4$  and 5 mM  $\beta$ -mercaptoethanol. Cell suspensions were sonicated and centrifuged at 10,000  $\times$  g for 30 min. CDK1 kinase activity condition was determined by using MV Peptide (CycLex Cdc2-Cyclin B kinase assay kit, Medical & Biological Laboratories Co Ltd, Nagoya, Japan) and measuring  $\text{OD}_{492}$  as described previously (42,43).

**Statistical analysis.** Our data were performed as means  $\pm$  SD of at least in triplicate. The difference between the AITC-treated

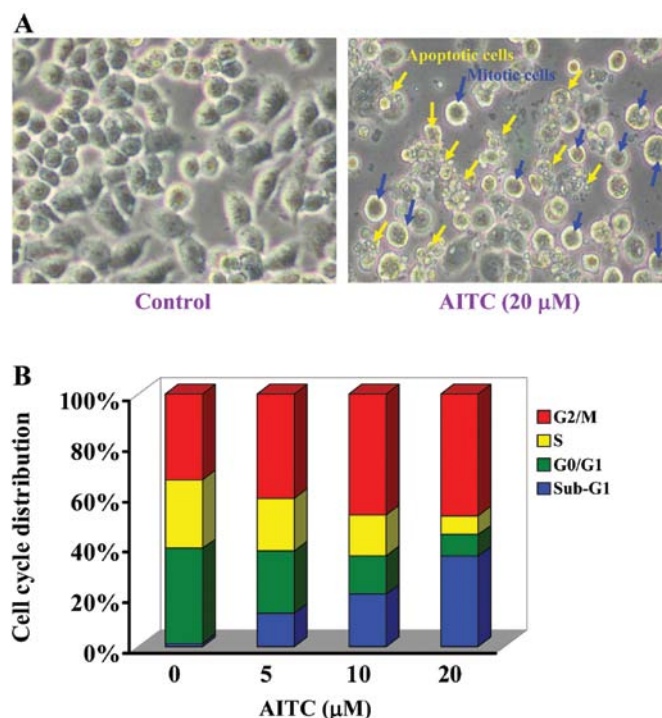


Figure 2. AITC promotes apoptosis and G<sub>2</sub>/M phase arrest in MDA-MB-468 cells. Cells were treated with or without 0, 5, 10 or 20  $\mu\text{M}$  of AITC for 24 h. (A) Cell morphology changes were observed (white arrows show apoptotic cells and black indicate mitotic cells) and photographed under phase-contrast microscopy at  $\times 200$  magnification. (B) Cells were analyzed for DNA content by a FACSCalibur flow cytometer as described in the Materials and methods. Data for cell cycle distribution show the percentage of total cells with DNA content (G<sub>2</sub>/M, S and G<sub>0</sub>/G<sub>1</sub> phases and sub-G<sub>1</sub> population). The data are representative of three independent experiments.

and control groups were analyzed by Student's t-test,  $p < 0.05$  was considered significant.

## Results

**AITC reduces cell viability and affects cell morphological changes and cell cycle arrest in MDA-MB-468 cells.** In order to examine the biological effects of AITC, MDA-MB-468 cells were treated with varying concentrations of AITC at 0, 5, 10 and 20  $\mu\text{M}$  for 24 and 48 h. Cells were harvested and the cell number was determined using trypan blue stain by Countess Automated Cell Counter, and the other cell viability and cell morphological changes were assayed by MTT and phase-contrast microscope. Fig. 1A shows that AITC time- and concentration-dependently decreased the number of MDA-MB-468 cells. Also, the results of these experiments indicated that AITC caused a decrease of cell viability (Fig. 1B) in a dose- and time-dependent manner as well as morphological changes (Fig. 2A). Based on these pilot observations, the treated concentrations were assessed for the effect of AITC at 5, 10 and 20  $\mu\text{M}$ , which caused strong induction of viable cells (Fig. 1B) and cell morphological changes (Fig. 2A) mostly in a dose- and time-dependent manner in 24 and 48 h. The half maximal inhibitory concentration ( $\text{IC}_{50}$ ) of AITC was  $10.26 \pm 1.31$   $\mu\text{M}$  after 24-h treatment. According to these results, the different concentration and cell death effects

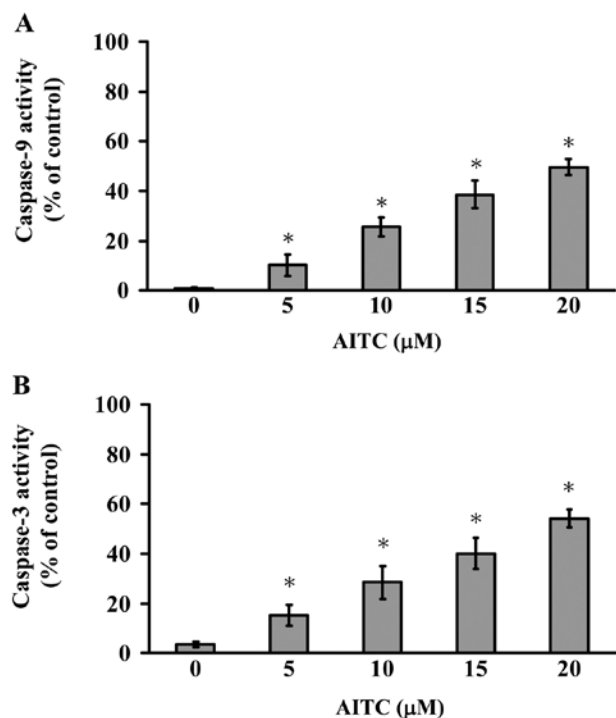


Figure 3. AITC enhances caspase-9 and caspase-3 activities in MDA-MB-468 cells. Cells were exposed to 0, 5, 10 or 20  $\mu\text{M}$  of AITC for 12 h. The whole-cell lysates were harvested as described in Materials and methods. (A) Caspase-9 and (B) caspase-3 activities were determined using the Caspase-9 and Caspase-3 Colorimetric assay kits. Results are presented as the mean  $\pm$  SD of three individual experiments. \* $p < 0.05$  indicates the level of significance compared with control (0  $\mu\text{M}$ ) value.

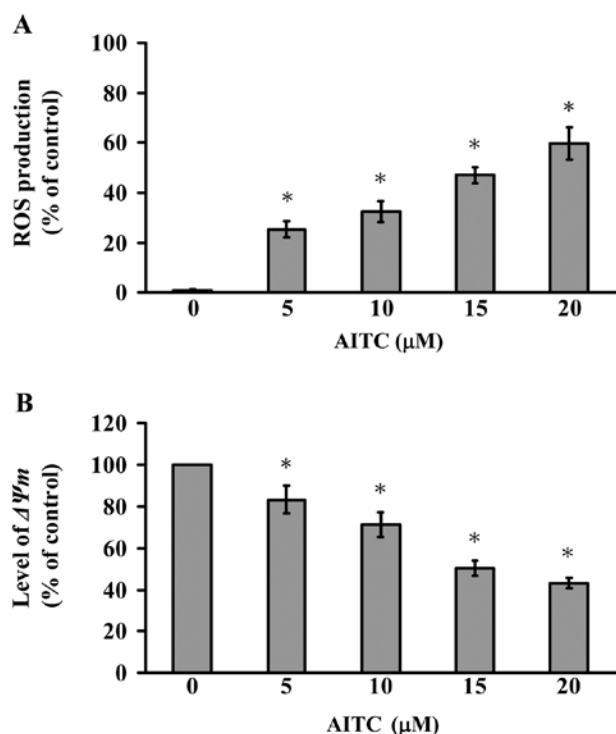


Figure 4. AITC stimulates ROS productions and decreases mitochondrial membrane potential ( $\Delta\Psi_m$ ) in MDA-MB-468 cells. Cells were incubated with 0, 5, 10 or 20  $\mu\text{M}$  of AITC for 12 h, and then harvested for examining the (A) ROS productions, (B) the level of  $\Delta\Psi_m$  as described in the Materials and methods. Data are shown as the mean  $\pm$  SD ( $n=3$ ) and significant difference (\* $p < 0.05$ ) was considered compared to the vehicle control (0  $\mu\text{M}$ ).

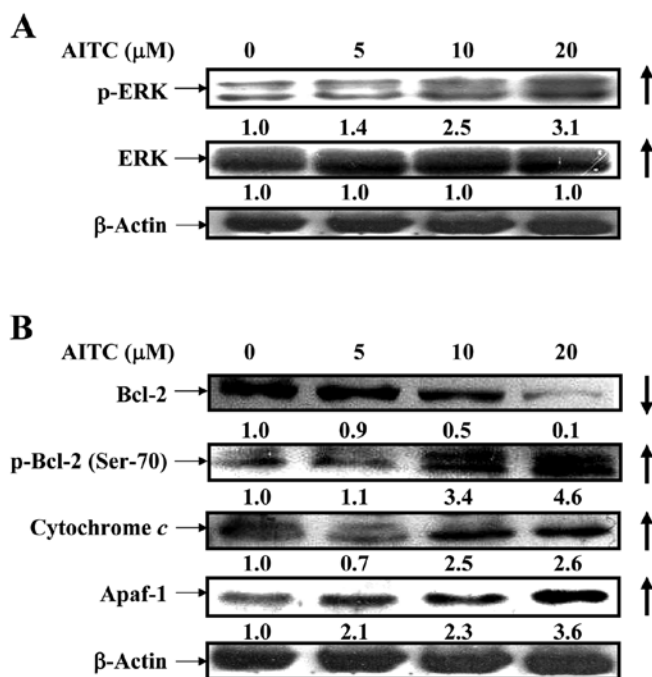


Figure 5. AITC alters the protein levels of ERK and intrinsic apoptotic signaling in MDA-MB-468 cells. Cells were treated with 0, 5, 10 or 20  $\mu\text{M}$  of AITC for 2 h (ERK and p-ERK protein levels) and 24 h. After treatment, cells were collected and lysed to subject to western blotting as described in Materials and methods. (A) Cell lysates were probed with anti-p-ERK and -ERK antibodies. (B) The protein levels of Bcl-2, p-Bcl-2 (Ser-70), cytochrome c and Apaf-1 expressions were examined.  $\beta$ -actin is an internal control and representative images were obtained from three independent experiments.

of AITC are accompanied by its effect on cell cycle progression and/or apoptotic cell death. We found that AITC promoted G<sub>2</sub>/M phase arrest and sub-G<sub>1</sub> population in MDA-MB-468 cells. Also, these effects were dose- and time-course dependent (Fig. 2B).

*AITC stimulates the activities of caspase-9 and -3 in MDA-MB-468 cells.* Cells were exposed to various concentrations of AITC for 12 h treatment to determine caspase-9 and -3 activities. Our results indicated that the caspase-9 and -3 activities were time- and concentration-dependently stimulated in AITC-treated MDA-MB-468 cells (Fig. 3). Thus, we suggest that AITC-triggered apoptosis is carried out through caspase-9 and -3-dependent signaling in MDA-MB-468 cells.

*AITC promotes the reactive oxygen species (ROS) production and loss of  $\Delta\Psi_m$  levels in MDA-MB-468 cells.* The results of flow cytometric analysis for ROS production and  $\Delta\Psi_m$  levels are shown in Fig. 4A and B. AITC-treated MDA-MB-468 cells with DCF were observed with increased intracellular ROS (Fig. 4A). We further explored if mitochondrial depolarization contributed to AITC-induced apoptosis of MDA-MB-468 cells. The treated and un-treated cells were exposed to AITC to investigate the change in  $\Delta\Psi_m$  in MDA-MB-468 after being stained with DiOC<sub>6</sub>(3), a mitochondria-specific and voltage-dependent dye. Results shown in Fig. 4B display that AITC significantly decreased the levels of  $\Delta\Psi_m$  in MDA-MB-468 cells (Fig. 4B). Based on these observations, we found that AITC-provoked cell

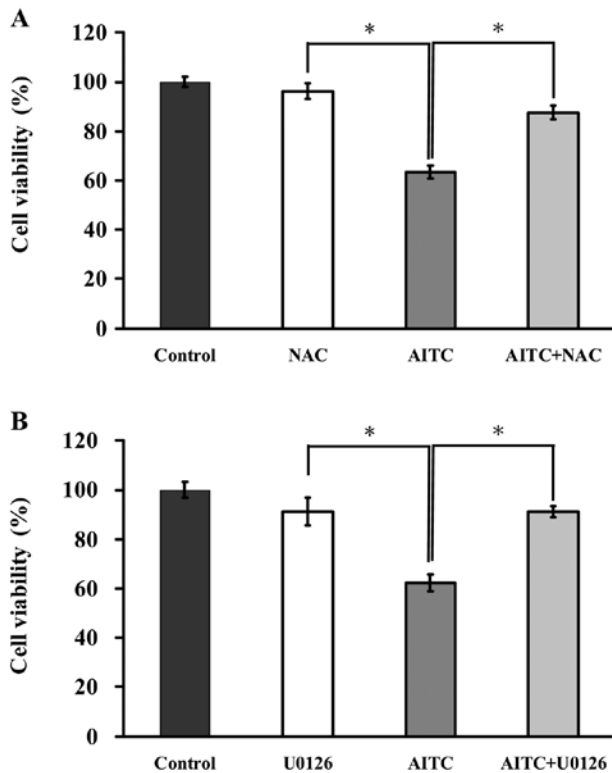


Figure 6. Effects of ROS and ERK contribute to AITC-reduced viability in MDA-MB-468 cells. Cells were pretreated with NAC (10 mM) and U0126 (10  $\mu$ M), respectively, and subsequently stimulated with 10  $\mu$ M AITC for 24 h. Cell viability was estimated by the MTT assay as described in the Materials and methods. Pre-incubation with (A) NAC and (B) U0126 to determine viability in AITC-treated MDA-MB-468 cells. Data are expressed as the mean  $\pm$  SD (n=3) and significant difference (\*p<0.05) was considered compared to the vehicle control (0  $\mu$ M).

apoptosis is involved in ROS production and intrinsic signaling pathway in MDA-MB-468 cells.

*AITC upregulates p-ERK signaling and alters mitochondria-dependent apoptotic pathway in MDA-MB-468 cells.* It is widely reported that ERK/MAPK positively regulated phosphorylation of Bcl-2 at Ser-70, causing antiapoptotic function to suppress Bcl-2 expression (44,45). To clarify whether AITC influences intrinsic apoptotic signaling through ERK pathway, the results from western blotting are shown in Fig. 5A and B indicating that the protein levels of p-ERK and ERK (Fig. 5A), p-Bcl-2 (Ser-70), cytochrome *c* and Apaf-1 (Fig. 5B) and p21/WAF-1 (Fig. 7B) were upregulated in MDA-MB-468 cells after treatment with AITC, but that of Bcl-2 was downregulated. Many reports have shown that apoptosis is associated with the loss of  $\Delta\Psi_m$  which is an endpoint of apoptosis (46). Our findings indicated that antiapoptosis signaling involving Bcl-2 phosphorylation is involved in ERK/MAPK pathway in AITC-treated MDA-MB-468 cells.

*ROS and ERK are associated with the induction of apoptosis in AITC-treated MDA-MB-468 cells.* To elucidate the possible signaling pathways of AITC-reduced viability of MDA-MB-468 cells, we determined whether ROS and ERK mediated AITC-regulated apoptotic signaling. Cells were pretreated with or without NAC (a ROS scavenger) and U0126

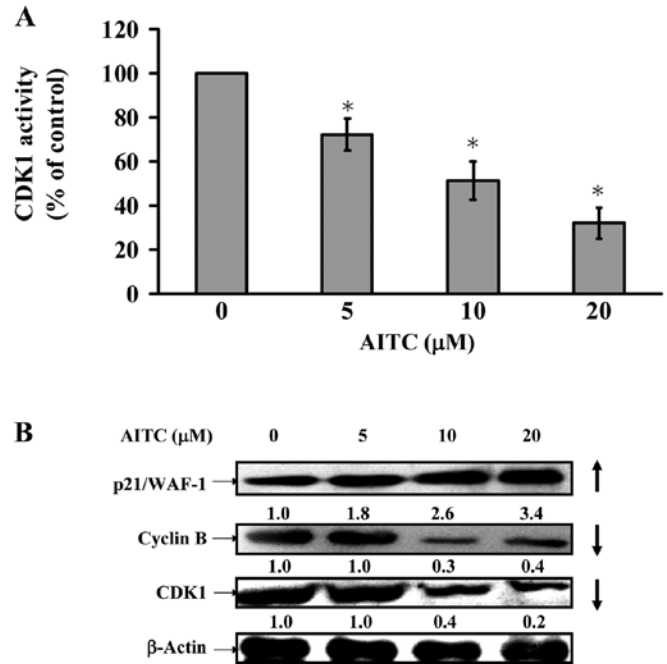


Figure 7. AITC reduces CDK1 activity and affects G<sub>2</sub>/M-associated protein levels in MDA-MB-468 cells. Cells were treated with 0, 5, 10 or 20  $\mu$ M of AITC for 12 h. (A) The CDK1 activity was determined utilizing CyclLex Cdc2-Cyclin B kinase assay kit (MBL International Corp.). Results represent the mean  $\pm$  SD (n=3). \*p<0.05 compared with the control (0  $\mu$ M) value. (B) The cell extracts were subjected to western blot analysis for the detection of p21/WAF-1, cyclin B and CDK1 expressions.  $\beta$ -actin was used as a loading control to ensure the same amount in each sample. Data were repeated and representative of three independent experiments with similar results.

(an ERK inhibitor) and then exposed to AITC (10  $\mu$ M) for 24 h. Cells were then determined for measuring cell viability by MTT assay. As shown in Fig. 6A, cells after treatment with AITC in presence and absence of NAC were observed to protect reduction of viability of MDA-MB-468 cells when compare with only AITC treated sample. Fig. 6B displays that reduction of cell viability in MDA-MB-468 cells by AITC was dramatically reversed by U0126 in comparison to AITC-treated only cells. Thus, ROS and ERK play central roles in AITC-induced apoptosis of MDA-MB-468 cells.

*AITC decreases CDK1 activity and alters G<sub>2</sub>/M phase-modulated protein levels in MDA-MB-468 cells.* We further assessed if G<sub>2</sub>/M phase arrest is involved in CDK1 activity, and data showed that AITC at 5-20  $\mu$ M dramatically reduced CDK1 activity in MDA-MB-468 cells (Fig. 7A). We also explored the possible molecular mechanisms in the modulation of G<sub>2</sub>/M phase arrest. Fig. 7B indicates that AITC caused an increase of p21/WAF-1 expression and a decrease of cyclin B and CDK1 protein levels in MDA-MB-468. Hence, we suggest that AITC-provoked G<sub>2</sub>/M phase arrest is mediated through activating p21/WAF-1 and suppressing CDK1/cyclin B expression in *in vitro* cultivation of MDA-MB-468 cells.

## Discussion

Many studies in new drug discovery have focused on breast adenocarcinoma therapeutic agents through the promotion

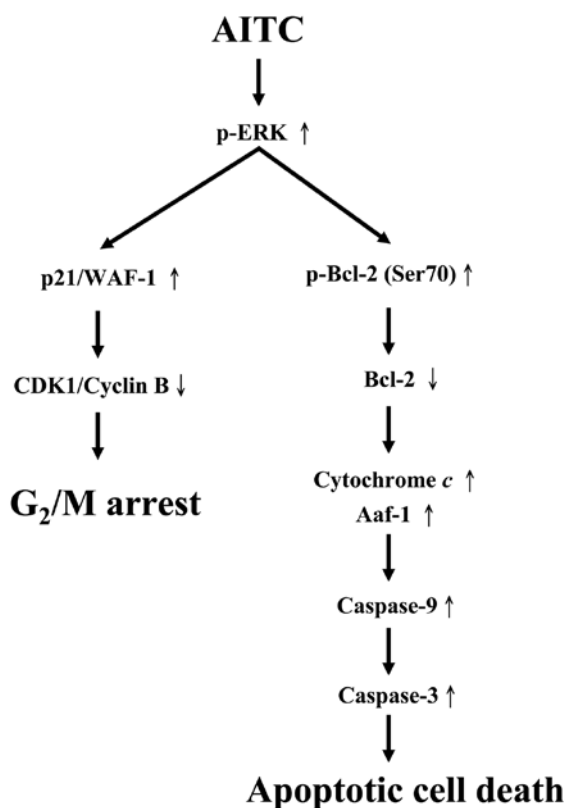


Figure 8. The proposed possible signaling pathways for AITC-induced  $G_2/M$  phase arrest through p21/WAF-1 and CDK1/cyclin B signaling and apoptosis via p-Bcl-2 (Ser70), mitochondria, caspase-9 and caspase-3-dependent pathways after activating phosphorylation of ERK in MDA-MB-468 cells.

of cell cycle arrest and induction of apoptotic cell death (47). Previous studies also demonstrated that AITC arrested HL60 leukemia cells at  $G_0/G_1$  phase (14), but caused  $G_2/M$  arrest in UMUC-3 cells (48), HeLa cells (13), HT29 cells (9), SW620 cells (15), GBM 8401 cells (16), PC-3 and LNCaP cells (49). In this study, our results showed that AITC inhibited the cell growth and proliferation on MCF-7 cells, MDA-MB-231 cells (data not shown), and MDA-MB-468 cells (Fig. 1) in a time- and concentration-dependent manner. The  $IC_{50}$  for 24-h treatment of AITC in MCF-7, MDA-MB-231 and MDA-MB-468 cells were  $17.96 \pm 2.58$ ,  $11.26 \pm 1.29$  and  $10.26 \pm 1.31 \mu M$ , respectively. One of the reasons for the differences in sensitivity in  $IC_{50}$  of different cell lines may be due to the inherently different doubling time in different cell lines. The doubling time of MCF-7, MDA-MB-231 and MDA-MB-468 cells were  $30.2 \pm 0.7$ ,  $28.1 \pm 1.2$  and  $29.9 \pm 0.5$  h (50). The distinct ability of AITC in growth inhibition of MCF-7, MDA-MB-231 and MDA-MB-468 cells might be caused by differential gene expression in different cell types. The MCF-7 cell line is p53 wild-type, but both of MDA-MB-231 and MDA-MB-468 cells are p53 mutant-type (51).

Many reports have shown that AITC-induced  $G_2/M$  arrest was associated with a marked decrease in the protein levels of cyclin B1, CDK1, cdc25B and cdc25C and caused the disruption of tubulin (9,52,53). The  $G_2/M$  phase progression is regulated with CDK1 kinases that are activated in association with cyclin A or cyclin B (52). The p21/WAF1 is one of the cyclin-dependent kinase inhibitors (CKI) which inhibits cyclin/CDK complexes in the  $G_2/M$  phase. The p21/WAF1 has been found to be associated

with the growth arrest in cells (53). Enhanced p21/WAF1 mRNA expression occurs through both p53-dependent and -independent mechanisms (54). Furthermore, ERK MAPK pathway has recently been reported to cooperate to cause sustained cell cycle arrest requiring p21/WAF1 expression (55,56). Our results from cell cycle analysis indicated that AITC induced  $G_2/M$  phase arrest (Fig. 2) in MDA-MB-468 cells. The CDK1 and cyclin B proteins were decreased (Fig. 7B), and phospho-ERK (Fig. 5A) and p21/WAF-1 (Fig. 7B) were increased by AITC treatment in a concentration-dependent manner. AITC also inhibited the CDK1 activity (Fig. 7A). Our study revealed that the novel molecular mechanism by which AITC induces  $G_2/M$  phase arrest and apoptosis in triple negative breast cancer MDA-MB-468 cells is through ERK-dependent p21/WAF-1 upregulation.

Two major signaling pathways are involved in apoptotic cell death (57,58). The extrinsic pathway (also called death receptor pathway) through the activation of the cell surface [Fas/Fas ligand (FasL) or TNF-related apoptosis-inducing ligand (TRAIL)] then promotes caspase-8 activation. The intrinsic pathway (also called mitochondria pathway) through death signals to mitochondria result in the release of mitochondrial inter-membrane proteins such as cytochrome *c*, which associate with apoptotic protease-activating factor-1 (Apaf-1) and pro-caspase-9 to form the apoptosome and then active caspase-3. The caspase-independent pathway is involved in the mitochondria which led to releases of apoptosis inducing factor (AIF) or endonuclease G (Endo G) from mitochondria causing cell death (59). Our results showed that AITC induced apoptotic death (sub- $G_1$  phase) of MDA-MB-468 cells and this action is concentration-dependent (Fig. 2B). AITC treatment in MDA-MB-468 cells concentration-dependently promoted the activations of caspase-9 and caspase-3 (Fig. 3). Cells were pretreated with NAC (a ROS scavenger) and U0126 (an ERK inhibitor) and exposed to AITC, leading to increase the percentage of viable cells when compared to the AITC-treated only cells (Fig. 6). The results in Fig. 5 show that the protein expressions of p-ERK, p-Bcl-2 (Ser-70), cytochrome *c* and Apaf-1 were upregulated in MDA-MB-468 cells after treatment with AITC. Our results suggested that AITC upregulated ERK signaling and altered mitochondria-dependent associated apoptotic pathway in MDA-MB-468 cells. Bcl-2 phosphorylation is known to affect antiapoptotic activity (44,45). Induction of apoptosis associated with Bcl-2 phosphorylation by anticancer agents has been linked with altering a variety of cellular signaling pathways, such as Ras/Raf, protein kinase C, protein kinase A, mitogen-activated protein kinase, ERK and CDK1 (35). Our results are in agreement with previous studies (60,61) indicating that that AITC-induced apoptotic cell death was caused by Bcl-2 phosphorylation and ERK activation.

The molecular signaling pathways are summarized in Fig. 8. Our results demonstrate that the ERK signaling pathway modulated intrinsic signaling and  $G_2/M$  phase arrest in AITC-treated MDA-MB-468 cells. These findings implied that AITC may be used as a novel therapeutic agent for the treatment of human breast cancer.

#### Acknowledgements

This study was supported by the grant CMU-100-ASIA-4 from China Medical University and partly supported by the Grant-

in-Aid from the National Science Council, Taiwan, R.O.C. (NSC 97-2320-B-039-004-MY3).

## References

- Kushad MM, Brown AF, Kurilich AC, *et al*: Variation of glucosinolates in vegetable crops of *Brassica oleracea*. *J Agric Food Chem* 47: 1541-1548, 1999.
- Rungapamestry V, Duncan AJ, Fuller Z and Ratcliffe B: Changes in glucosinolate concentrations, myrosinase activity, and production of metabolites of glucosinolates in cabbage (*Brassica oleracea* var. capitata) cooked for different durations. *J Agric Food Chem* 54: 7628-7634, 2006.
- Uematsu Y, Hirata K, Suzuki K, Iida K, Ueta T and Kamata K: Determination of isothiocyanates and related compounds in mustard extract and horseradish extract used as natural food additives. *Shokuhin Eiseigaku Zasshi* 43: 10-17, 2002 (In Japanese).
- Zhang Y: Allyl isothiocyanate as a cancer chemopreventive phytochemical. *Mol Nutr Food Res* 54: 127-135, 2010.
- Negri R, Muntoni F and D'Amore R: Antibiotic effect of the allyl isothiocyanate extracted from various horticultural forms of the seeds of *Raphanus Sativus L.* var. radicola pers. towards various bacteria, including two strains of tubercle bacillus avian type, Cow 18 and Cow 70; Note II. *Rend Ist Sup Sanit* 14: 186-193, 1951.
- Wagner AE, Boesch-Saadatmandi C, Dose J, Schultheiss G and Rimbach G: Anti-inflammatory potential of allyl-isothiocyanate - role of Nrf2, NF-(kappa) B and microRNA-155. *J Cell Mol Med* 16: 836-843, 2012.
- Sellam A, Dongo A, Guillemette T, Hudhomme P and Simoneau P: Transcriptional responses to exposure to the brassicaceous defence metabolites camalexin and allyl-isothiocyanate in the necrotrophic fungus *Alternaria brassicicola*. *Mol Plant Pathol* 8: 195-208, 2007.
- Srivastava SK, Xiao D, Lew KL, *et al*: Allyl isothiocyanate, a constituent of cruciferous vegetables, inhibits growth of PC-3 human prostate cancer xenografts in vivo. *Carcinogenesis* 24: 1665-1670, 2003.
- Smith TK, Lund EK, Parker ML, Clarke RG and Johnson IT: Allyl-isothiocyanate causes mitotic block, loss of cell adhesion and disrupted cytoskeletal structure in HT29 cells. *Carcinogenesis* 25: 1409-1415, 2004.
- Smith T, Musk SR and Johnson IT: Allyl isothiocyanate selectively kills undifferentiated HT29 cells in vitro and suppresses aberrant crypt foci in the colonic mucosa of rats. *Biochem Soc Trans* 24: 381S, 1996.
- Bhattacharya A, Li Y, Geng F, Munday R and Zhang Y: The principal urinary metabolite of allyl isothiocyanate, N-acetyl-S-(N-allylthiocarbamoyl)cysteine, inhibits the growth and muscle invasion of bladder cancer. *Carcinogenesis* 33: 394-398, 2012.
- Bhattacharya A, Tang L, Li Y, *et al*: Inhibition of bladder cancer development by allyl isothiocyanate. *Carcinogenesis* 31: 281-286, 2010.
- Hasegawa T, Nishino H and Iwashima A: Isothiocyanates inhibit cell cycle progression of HeLa cells at G2/M phase. *Anticancer Drugs* 4: 273-279, 1993.
- Zhang Y, Tang L and Gonzalez V: Selected isothiocyanates rapidly induce growth inhibition of cancer cells. *Mol Cancer Ther* 2: 1045-1052, 2003.
- Lau WS, Chen T and Wong YS: Allyl isothiocyanate induces G<sub>2</sub>/M arrest in human colorectal adenocarcinoma SW620 cells through downregulation of Cdc25B and Cdc25C. *Mol Med Rep* 3: 1023-1030, 2010.
- Chen NG, Chen KT, Lu CC, *et al*: Allyl isothiocyanate triggers G<sub>2</sub>/M phase arrest and apoptosis in human brain malignant glioma GBM 8401 cells through a mitochondria-dependent pathway. *Oncol Rep* 24: 449-455, 2010.
- Hwang ES and Lee HJ: Allyl isothiocyanate and its N-acetylcysteine conjugate suppress metastasis via inhibition of invasion, migration, and matrix metalloproteinase-2/-9 activities in SK-Hep 1 human hepatoma cells. *Exp Biol Med* (Maywood) 231: 421-430, 2006.
- Rodrigues-Ferreira S, Abdelkarim M, Dillenburg-Pilla P, *et al*: Angiotensin II facilitates breast cancer cell migration and metastasis. *PLoS One* 7: e35667, 2012.
- Jemal A, Bray F, Center MM, Ferlay J, Ward E and Forman D: Global cancer statistics. *CA Cancer J Clin* 61: 69-90, 2011.
- Ossovskaya V, Wang Y, Budoff A, *et al*: Exploring molecular pathways of triple-negative breast cancer. *Genes Cancer* 2: 870-879, 2011.
- Rakha EA, Reis-Filho JS and Ellis IO: Basal-like breast cancer: a critical review. *J Clin Oncol* 26: 2568-2581, 2008.
- Gucalp A and Traina TA: Triple-negative breast cancer: adjuvant therapeutic options. *Chemother Res Pract* 2011: 696208, 2011.
- Gelman K, Dent R, Mackey JR, Laing K, McLeod D and Verma S: Targeting triple-negative breast cancer: optimising therapeutic outcomes. *Ann Oncol*: Apr 19, 2012 (Epub ahead of print).
- Li C, Zhao X, Toline EC, *et al*: Prevention of carcinogenesis and inhibition of breast cancer tumor burden by dietary stearate. *Carcinogenesis* 32: 1251-1258, 2011.
- Ebert T, Kleine-Gunk B, Altwein JE, Miller K and Mallmann P: Dietary prevention of carcinomas of the breast and prostate: fundamental and practical aspects of the Nutritional Cancer Prevention (NCP) program. *Dtsch Med Wochenschr* 127: 1392-1396, 2002 (In German).
- Chen KT, Hour MJ, Tsai SC, *et al*: The novel synthesized 6-fluoro-(3-fluorophenyl)-4-(3-methoxyanilino)quinazoline (LJJ-10) compound exhibits anti-metastatic effects in human osteosarcoma U-2 OS cells through targeting insulin-like growth factor-I receptor. *Int J Oncol* 39: 611-619, 2011.
- Liao CL, Lai KC, Huang AC, *et al*: Gallic acid inhibits migration and invasion in human osteosarcoma U-2 OS cells through suppressing the matrix metalloproteinase-2/-9, protein kinase B (PKB) and PKC signaling pathways. *Food Chem Toxicol* 50: 1734-1740, 2012.
- Yu FS, Wu CC, Chen CT, *et al*: Diallyl sulfide inhibits murine WEHI-3 leukemia cells in BALB/c mice in vitro and in vivo. *Hum Exp Toxicol* 28: 785-790, 2009.
- Tsou MF, Peng CT, Shih MC, *et al*: Benzyl isothiocyanate inhibits murine WEHI-3 leukemia cells in vitro and promotes phagocytosis in BALB/c mice in vivo. *Leuk Res* 33: 1505-1511, 2009.
- Lu CC, Yang JS, Huang AC, *et al*: Chrysophanol induces necrosis through the production of ROS and alteration of ATP levels in J5 human liver cancer cells. *Mol Nutr Food Res* 54: 967-976, 2010.
- Lu CC, Yang JS, Chiang JH, *et al*: Novel quinazolinone MJ-29 triggers endoplasmic reticulum stress and intrinsic apoptosis in murine leukemia WEHI-3 cells and inhibits leukemic mice. *PLoS One* 7: e36831, 2012.
- Lin JP, Yang JS, Chang NW, *et al*: GADD153 mediates berberine-induced apoptosis in human cervical cancer Ca ski cells. *Anticancer Res* 27: 3379-3386, 2007.
- Lin YT, Yang JS, Lin HJ, *et al*: Baicalein induces apoptosis in SCC-4 human tongue cancer cells via a Ca<sup>2+</sup>-dependent mitochondrial pathway. *In Vivo* 21: 1053-1058, 2007.
- Ying WZ and Sanders PW: Cytochrome c mediates apoptosis in hypertensive nephrosclerosis in Dahl/Rapp rats. *Kidney Int* 59: 662-672, 2001.
- Yang JS, Hour MJ, Huang WW, Lin KL, Kuo SC and Chung JG: MJ-29 inhibits tubulin polymerization, induces mitotic arrest, and triggers apoptosis via cyclin-dependent kinase 1-mediated Bcl-2 phosphorylation in human leukemia U937 cells. *J Pharmacol Exp Ther* 334: 477-488, 2010.
- Liu KC, Huang AC, Wu PP, *et al*: Gallic acid suppresses the migration and invasion of PC-3 human prostate cancer cells via inhibition of matrix metalloproteinase-2 and -9 signaling pathways. *Oncol Rep* 26: 177-184, 2011.
- Lan YH, Wu YC, Wu KW, *et al*: Death receptor 5-mediated TNFR family signaling pathways modulate  $\gamma$ -humulene-induced apoptosis in human colorectal cancer HT29 cells. *Oncol Rep* 25: 419-424, 2011.
- Wu SH, Hang LW, Yang JS, *et al*: Curcumin induces apoptosis in human non-small cell lung cancer NCI-H460 cells through ER stress and caspase cascade- and mitochondria-dependent pathways. *Anticancer Res* 30: 2125-2133, 2010.
- Lai WW, Yang JS, Lai KC, *et al*: Rhein induced apoptosis through the endoplasmic reticulum stress, caspase- and mitochondria-dependent pathways in SCC-4 human tongue squamous cancer cells. *In Vivo* 23: 309-316, 2009.
- Chiang JH, Yang JS, Ma CY, *et al*: Danthron, an anthraquinone derivative, induces DNA damage and caspase cascade-mediated apoptosis in SNU-1 human gastric cancer cells through mitochondrial permeability transition pores and Bax-triggered pathways. *Chem Res Toxicol* 24: 20-29, 2011.

41. Huang WW, Chiu YJ, Fan MJ, *et al*: Kaempferol induced apoptosis via endoplasmic reticulum stress and mitochondria-dependent pathway in human osteosarcoma U-2 OS cells. *Mol Nutr Food Res* 54: 1585-1595, 2010.
42. Huang WW, Ko SW, Tsai HY, *et al*: Cantharidin induces G<sub>2</sub>/M phase arrest and apoptosis in human colorectal cancer colo 205 cells through inhibition of CDK1 activity and caspase-dependent signaling pathways. *Int J Oncol* 38: 1067-1073, 2011.
43. Chou LC, Yang JS, Huang LJ, *et al*: The synthesized 2-(2-fluorophenyl)-6,7-methylenedioxyquinolin-4-one (CHM-1) promoted G<sub>2</sub>/M arrest through inhibition of CDK1 and induced apoptosis through the mitochondrial-dependent pathway in CT-26 murine colorectal adenocarcinoma cells. *J Gastroenterol* 44: 1055-1063, 2009.
44. Deng X, Kornblau SM, Ruvolo PP and May WS Jr: Regulation of Bcl2 phosphorylation and potential significance for leukemic cell chemoresistance. *J Natl Cancer Inst Monogr* 30-37, 2001.
45. Mai H, May WS, Gao F, Jin Z and Deng X: A functional role for nicotine in Bcl2 phosphorylation and suppression of apoptosis. *J Biol Chem* 278: 1886-1891, 2003.
46. Lavrik IN, Golks A and Krammer PH: Caspases: pharmacological manipulation of cell death. *J Clin Invest* 115: 2665-2672, 2005.
47. Choi JA, Kim JY, Lee JY, *et al*: Induction of cell cycle arrest and apoptosis in human breast cancer cells by quercetin. *Int J Oncol* 19: 837-844, 2001.
48. Tang L and Zhang Y: Dietary isothiocyanates inhibit the growth of human bladder carcinoma cells. *J Nutr* 134: 2004-2010, 2004.
49. Xiao D, Srivastava SK, Lew KL, *et al*: Allyl isothiocyanate, a constituent of cruciferous vegetables, inhibits proliferation of human prostate cancer cells by causing G<sub>2</sub>/M arrest and inducing apoptosis. *Carcinogenesis* 24: 891-897, 2003.
50. Watanabe N, Okochi E, Mochizuki M, Sugimura T and Ushijima T: The presence of single nucleotide instability in human breast cancer cell lines. *Cancer Res* 61: 7739-7742, 2001.
51. Salem SD, Abou-Tarboush FM, Saeed NM, *et al*: Involvement of p53 in gemcitabine mediated cytotoxicity and radiosensitivity in breast cancer cell lines. *Gene* 498: 300-307, 2012.
52. Lobrich M and Jeggo PA: The impact of a negligent G<sub>2</sub>/M checkpoint on genomic instability and cancer induction. *Nat Rev Cancer* 7: 861-869, 2007.
53. Maeda T, Nagaoka Y, Kawai Y, *et al*: Inhibitory effects of cancer cell proliferation by novel histone deacetylase inhibitors involve p21/WAF1 induction and G<sub>2</sub>/M arrest. *Biol Pharm Bull* 28: 849-853, 2005.
54. Wu L and Levine AJ: Differential regulation of the p21/WAF-1 and mdm2 genes after high-dose UV irradiation: p53-dependent and p53-independent regulation of the mdm2 gene. *Mol Med* 3: 441-451, 1997.
55. Ciccarelli C, Marampon F, Scoglio A, *et al*: p21WAF1 expression induced by MEK/ERK pathway activation or inhibition correlates with growth arrest, myogenic differentiation and onco-phenotype reversal in rhabdomyosarcoma cells. *Mol Cancer* 4: 41, 2005.
56. Lee B and Moon SK: Ras/ERK signaling pathway mediates activation of the p21WAF1 gene promoter in vascular smooth muscle cells by platelet-derived growth factor. *Arch Biochem Biophys* 443: 113-119, 2005.
57. Kroemer G, Galluzzi L and Brenner C: Mitochondrial membrane permeabilization in cell death. *Physiol Rev* 87: 99-163, 2007.
58. Lai E, Teodoro T and Volchuk A: Endoplasmic reticulum stress: signaling the unfolded protein response. *Physiology (Bethesda)* 22: 193-201, 2007.
59. Park HH: Structural features of caspase-activating complexes. *Int J Mol Sci* 13: 4807-4818, 2012.
60. Geng F, Tang L, Li Y, *et al*: Allyl isothiocyanate arrests cancer cells in mitosis, and mitotic arrest in turn leads to apoptosis via Bcl-2 protein phosphorylation. *J Biol Chem* 286: 32259-32267, 2011.
61. Xu C, Shen G, Yuan X, *et al*: ERK and JNK signaling pathways are involved in the regulation of activator protein 1 and cell death elicited by three isothiocyanates in human prostate cancer PC-3 cells. *Carcinogenesis* 27: 437-445, 2006.